Engineering Structures 228 (2021) 111565

Contents lists available at ScienceDirect

Engineering Structures

journal homepage: www.elsevier.com/locate/engstruct

Span-to-depth ratio limits for RC continuous beams and slabs based on MC2010 and EC2 ductility and deflection requirements

José Santos [a,c,*], António Abel Henriques [b,c]

[a] UMa – University of Madeira, FCEE – Faculty of Exact Sciences and Engineering, DECG – Department of Civil Engineering and Geology, 9020-105 Funchal, Portugal
[b] University of Porto, Faculty of Engineering, Department of Civil Engineering, 4200-465 Porto, Portugal
[c] CONSTRUCT-LABEST, Faculty of Engineering (FEUP), University of Porto, Portugal

ARTICLE INFO

Keywords:
Continuous beams
Continuous slabs
Deflection control
Deflection ductility index
Eurocode 2
Model Code 2010
Pre-design
Required ductility
Rotation capacity
Slenderness ratio

ABSTRACT

In the design of reinforced concrete structures several limit states are usually verified using simplified methods instead of using complex direct calculation. Span-to-depth ratio limits are applied for deflection control. In the same way, a redistribution factor and the relative depth of the compression zone are applied for the required ductility, but this is not enough. In fact, specific span-to-depth ratio limits, which are developed in this paper, should also complement the conditions referred to here.

A numerical study is developed to compute the deflection ductility index of a wide range of continuous beams (or one-way slabs) considering as ultimate point when the rotation capacity (given by MC2010 and EC2) is achieved. From the boundary between fragile and ductile failures, the new span-to-depth ratio limits for the required ductility are defined and compared with the existing similar limits for deflection control.

The results indicate that: (i) for normal strength concrete (up to 50 MPa), the ductility limit is more restrictive than the deflection limit when the redistribution factor δ is lower than 0.9, being always more restrictive for high strength concrete; (ii) for the current building beams, the slenderness used ($10 < l/d < 20$) allows ductile failures, while for typical building slabs (low reinforcement ratio, but high redistribution), the slenderness should be $l/d \leq 20$; (iii) the conditions of MC2010 and EC2 to use plastic analysis without any direct check of the rotation capacity are actually incomplete and need to be revised.

The new span-to-depth ratio limits proposed in this paper, which satisfy both ductility and deflection requirements, depend on the redistribution factor, characteristic compressive strength of concrete and total mechanical reinforcement ratio.

1. Introduction

As reinforced concrete (RC) is the most used construction material in the world, the scientific knowledge about it has increased greatly during recent decades. Nowadays, the design of a simple RC structure includes several tasks, with many calculations and parameters, the reason why using computers is now almost mandatory. In this context, the demand from structural engineers for simplified design methods has grown, at least for pre-designing the RC elements.

The simplified design methods make it possible, with simple considerations, to define solutions which permit one Ultimate Limit State (ULS) or one Serviceability Limit State (SLS) to be fulfilled, avoiding the complex calculations of that limit state. Taking into account their popularity, several RC codes (like the two used here: MC2010 [1] and EC2 [2]) already include these simplified methods. To define these, several assumptions about the expected behaviour of the RC structure and the loading are considered, which may sometimes not be true. This is why the codes usually only present simplified design methods for the SLS, because the target reliability index is significantly lower than the values defined for the ULS. Thus, it is common to find simplified design methods for crack control, deflection control and vibration control.

Regarding deflection control, several methodologies were proposed to estimate the deflection of RC beams [3,4] and slabs [5], depending mainly on the loading, quantity of reinforcement, geometry, creep and shrinkage. However, a simplified method based on the span-to-depth (or slenderness) ratio limit was developed. During last decades, based on different approaches, several researchers proposed their formulas for span-to-depth ratio limits. Some of these limits are now in codes, and

* Corresponding author.
E-mail address: jmmns@fe.up.pt (J. Santos).

https://doi.org/10.1016/j.engstruct.2020.111565
Received 18 June 2020; Received in revised form 6 November 2020; Accepted 9 November 2020
Available online 7 December 2020

depend mainly on the structural system, the type of element and the concrete strength class. This methodology has been applied with success for many years. Gardner [6], Lee et al. [7], Veselin & Rumen [8] and Eren et al. [9] compared the limits of several known RC codes (ACI 318, MC2010/EC2, CSA A23.3, AS 3600) and proposals of numerous researchers. As they conclude that code limits do not always give conservative results, some corrections were proposed. Similar methodology was developed for slabs [10] and prestressed beams [11]. Besides these previous knowledge, more recently, complex formulas were proposed by Scanlon & Lee [12] and Caldentey et al. [13], exclusively to control deflection, and Marí et al. [14] to control not only deflection but also crack width, both related to SLS. Note that, none of known slenderness limit includes any ULS.

However, from the ULS it is also possible to define span-to-depth ratio limits, as developed in this paper, from the required ductility. In fact, the ductility of RC structures is an essential property not only to accommodate the change that occurs in the deformation field during its service lifetime, but also to ensure that statically indeterminate structures have a plastic behaviour during rupture, which means that engineers can apply plastic design. The ductility can be evaluated at different levels: materials, cross-sections and elements, with the respective number of influential parameters successively growing. The last one, ductility in elements, being a global ductility factor, is used in this paper.

In this sense, drift ratio limits are generally used for reinforced concrete columns. Matamoros et al. [15], Lam et al. [16], Rodrigues et al. [17], Wibowo et al. [18], Zoppo et al. [19], Raza et al. [20] performed several experimental tests to investigate the behaviour of columns subjected to cyclic loadings. The most significant parameters for the drift ratio, such as the axial load level, amount of transverse reinforcement, slenderness of the column, and the yield strength of the longitudinal reinforcement, were identified. Sindel et al. [21] compared the drift limits of several codes. Erduran & Yakut [22] and Lu et al. [23] performed numerical analysis to evaluate the drift limits of RC columns. Empirical equations to describe the drift ratio limits were proposed. This visual reading is usually presented as a function of the damage limit, slenderness, class and quantity of reinforcement and axial load level. Other studies on columns calculated the ductility factors [16,24]. However, according to Lam et al. [16], the performance of columns may not be accurately expressed by the section ductility factor, but a better representation could be achieved by using the drift ratio (a global ductility factor). This conclusion is relevant because on beams global ductility factors usually are not used.

In fact, the study of ductility on beams is typically restricted to the calculation of the rotation capacity of the plastic hinges (a local ductility factor) in order to estimate the allowable degree of moment redistribution. CEB Task Group 2.2 bulletins [25] and [26] include several works and a synthesis about RC ductility, rotation capacity and moment redistribution. Bernardo & Lopes [27], Bagge et al. [28], Sin et al. [29], Carmo [30], Shin et al. [31] and Bernardo et al. [32] performed experimental tests and extended this knowledge for other types of concrete. Salvatore et al. [33] did the same for a specific type of steel. Farouk & Khalil [34], Pokhrel & Bandelt [35], Carpinteri & Corrado [36] and Erduran E, Yakut [37] present several numerical studies to estimate the ductility of RC beams. From all this experimental, theoretical and numerical studies, the influence on the ductility of the geometry, materials properties, structural system, reinforcement (longitudinal and transverse), and loading (monotonic and reversed cyclic) was identified and quantified.

Therefore, in contrast with RC columns, in RC beams and slabs global ductility factors are not usually used, as developed in this paper. However, the deflection ductility index on beams and slabs can be a useful tool for designers because it represents how much a beam can deform after maximum load. When this index is lower than one, a fragile and premature rupture occurs, and the maximum load is lower than the theoretical plastic capacity of the beam. To avoid that, the deflection ductility index should be equal to or higher than one. This condition leads to a span-to-depth ratio limit, which could also be used in pre-design, in the same way as it is used for deflection control. For this reason, it could be a good tool for RC structural pre-design. According to the authors' knowledge, this has never previously been done.

Thus, in this paper the span-to-depth ratio limits for continuous beams (or one-way continuous slabs, or two-way spanning slabs continuous over one long side) based on the required ductility are calculated from the deflection ductility index, which constitutes the main novelty of this paper. Afterwards, these limits are compared with similar deflection control limits to find the most conditioning one. To be consistent, the assumptions of *fib* Model Code 2010 - Volume 2 [1] (similar to the Eurocode 2 - Part 1-1: 2004 [2]) are applied for both requirements.

To achieve this, in Section 2 a brief explanation of the behaviour of continuous RC one-way members is done, the fundamental parameters and the rupture criterion are introduced, and the numerical study and the numerical model to compute the deflection ductility index are described. In Section 3, the results of the deflection ductility index are first presented, then from these the span-to-depth ratio limits are derived and compared with the deflection span-to-depth ratio limits, and lastly new equations for span-to-depth ratio limits are proposed. Section 4 presents the main conclusions.

2. Concepts and methodology

2.1. Behaviour of continuous RC one-way members up to rupture

Continuous RC beams or one-way spanning slabs show a marked non-linear behaviour with the increase of loading. Fig. 1 presents a simplified model for an interior span with a rectangular cross-section submitted to a uniformly distributed load up to rupture. The deflection response of the beam under loading can be explained approximately by the graph illustrated in Fig. 2a) with four different lines delimited by the origin and four characteristic zones.

For low actions all beam sections remain uncracked with the full stiffness. Cracking at the continuous supports takes place in Zone 1, followed by cracking in the span. The load continues to increase considerably until the reinforcing bars at the supports reach the yielding (Zone 2). At the supports, plastic hinges are developed, and they start to rotate under more loading.

If the structure has enough ductility, in Zone 3 a new yielding occurs on the reinforcing bars at the mid-span and a new plastic hinge is created at this section. With three plastic hinges a collapse mechanism is formed, which means that the loading capacity of the beam has been reached. From this zone, small load increments cause large deflections. When the rotation capacity of the plastic hinges located at the supports is attained (Zone 4), the beam collapses and the load capacity is lost.

However, if the structure has limited ductility (Fig. 2b)), Zones 3 and 4 cannot be achieved, and a premature collapse may occur. This means that the plastic hinges in the supports have achieved their capacity before the development of the plastic hinge in the mid-span. In this situation, the full capacity of the element (beam or slab) is lower than the design value obtained by the plastic analysis. To avoid that, at least Zone 3 should be achieved.

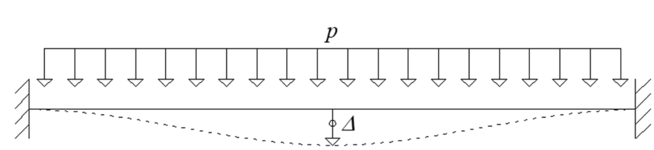

Fig. 1. Simplified model for an interior span of a continuous beam or one-way spanning slab under uniformly distributed load and its mid-span deflection.

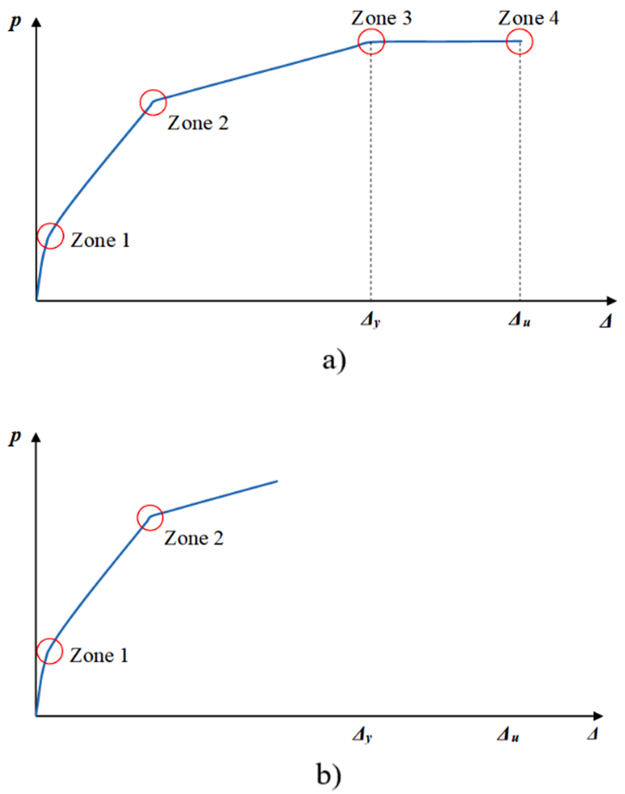

Fig. 2. Loading versus mid-span deflection curve: (a) with enough ductility, (b) without ductility.

2.2. Basic parameters and rupture criterion

Regarding the bending ductility of RC structures, it is important to remember three parameters: μ_Δ, δ and θ_{pl}. The deflection ductility index μ_Δ is defined as the ratio between the ultimate deflection Δ_u and yield deflection Δ_y of beams (Eq. (1)). The objective of this paper is to provide elements whose span-to-depth ratio ensures that Zone 3 is always reached, that is, the element achieves its full capacity; this means that μ_Δ should be equal to or higher than one.

The redistribution factor δ (Eq. (2)) is defined as the ratio between the support bending moment after redistribution ($M_{sup,red}$) and the support bending moment calculated according to the theory of elasticity ($M_{sup,el}$) or without any redistribution.

$$\mu_\Delta = \frac{\Delta_u}{\Delta_y} \tag{1}$$

$$\delta = \frac{M_{sup,red}}{M_{sup,el}} \tag{2}$$

In numerical studies the yield deflection Δ_y is usually easier to calculate than the ultimate deflection Δ_u because the first occurs when yielding is detected and the second depends on the rupture criterion used, which in turn depends on the type of analysis which is performed (Bernoulli beam, plane stress, volumetric). In this paper an analysis with Bernoulli beams is carried out (Section 2.3), so the most appropriate rupture criterion is through the rotation capacity (of plastic hinges in supports). As mentioned in Section 2.1, when the rotation capacity of the plastic hinges located at the supports is attained, it is considered that ultimate deflection Δ_u is achieved.

The total rotation θ is equal to the sum of curvature along the member length at failure, while the elastic rotation θ_{el} is defined at the onset of yielding of reinforcement [26]. The rotation capacity is understood as the maximum plastic rotation θ_{pl} of two sections and it is calculated as the difference between the total rotation at failure θ and the elastic rotation at the onset of yielding of reinforcement θ_{el}. Fig. 3 shows the definition of plastic rotation according to the CEB [26].

Regarding the calculation of the rotation capacity on beams and slabs, there are several models recognised by the international scientific community of structural engineering that present good results. These include the Stuttgart model, Naples model, Darmstadt-Leipzig model, Zürich model, Delft model (all detailed in [26]), Coimbra model [38], Adelaide model [39] and Hong Kong model [40]. Although these models show different results and the experimental results indicate some dispersion, in general the values of rotation capacity predicted by the different models are similar and they compare well with the experimental results [26,40]. For columns with axial forces and cyclic loadings, other models should be used, like the Salerno model [41].

Considering these models and the existing experimental data, the rotation capacities have been established in several codes. From these codes, the simplified procedure defined by *fib* Model Code 2010 – Volume 2 (MC2010) [1] and Eurocode 2 - Part 1–1: 2004 (EC2) [2] is the one that gives the most reasonable results [42]. Therefore, in this paper we apply this procedure, which states not only the rotation capacity of continuous beams or one-way spanning slabs, but also the conditions for its application.

This procedure is based on the rotation capacity of a beam or one-way spanning slab zone over a length of approximately 1.2 times the section depth (Fig. 4). It is assumed that these zones are subjected to a plastic deformation (formation of plastic hinges) under the relevant combination of actions [2]. The basic value $\theta_{pl,basic}$ for the rotation capacity according to this procedure is shown in Fig. 5 for reinforcing steel class C. To take into account the shear slenderness, the basic value $\theta_{pl,basic}$ should be adjusted according to Eq. (3). Therefore, the main parameters for rotation capacity θ_{pl} in this procedure are the relative depth of the compression zone x/d and the shear slenderness $M_{Sd}/V_{Sd}.d$.

$$\theta_{pl} = \theta_{pl,basic} \cdot \sqrt{\frac{M_{Sd}}{3 \cdot V_{Sd} \cdot d}} \tag{3}$$

where: M_{Sd} is the design value of the applied bending moment over the support; V_{Sd} is the design value of the applied shear force near the support; d is the effective depth of the cross-section.

2.3. Numerical study

As explained in Section 2.2, the deflection ductility index μ_Δ can

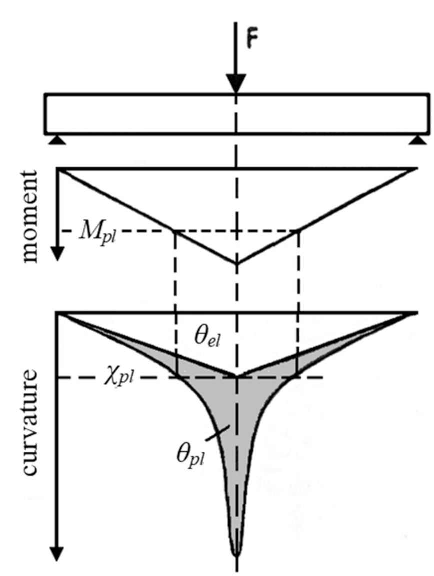

Fig. 3. Definition of plastic rotation according to the CEB [26].

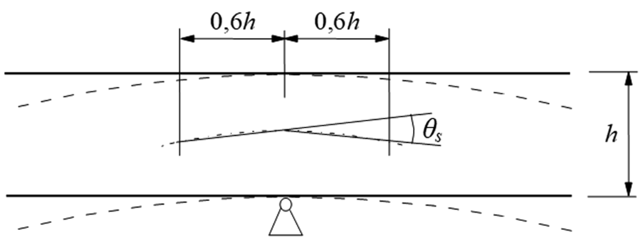

Fig. 4. Geometry definition of a plastic hinge in MC2010 and EC2.

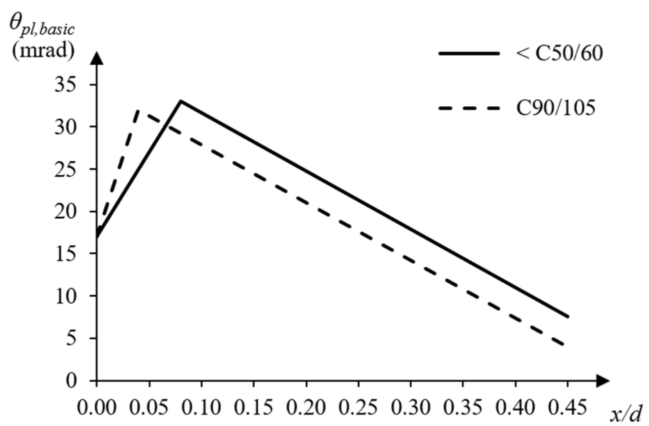

Fig. 5. Basic value of rotation capacity in MC2010 and EC2 for reinforcing steel class C.

distinguish safe cases from unsafe cases when its value is larger or smaller than one. From the boundary line between the two cases ($\mu_\Delta = 1$), it is possible to define the span-to-depth ratio limits based on the required ductility. Thus, the deflection ductility index is first numerically calculated and from these results the span-to-depth ratio limits are defined.

Therefore, a systematic analysis is developed with the objective of quantifying the deflection ductility index. The variation of the deflection ductility index was obtained by taking into account the variation of the six parameters defined in Table 1. Each parameter can have different values according to Table 1. All 324 combinations of these values were processed.

Initially the section width was introduced as a parameter, but it was noticed that this parameter did not change the results, because the mechanical reinforcement ratio ω^t includes this parameter. The chosen values for span l, effective depth d and mechanical reinforcement ratio ω^t include most of the common beams used in building construction. For the redistribution factor δ, the three most typical situations were selected: $\delta = 1.0$ represents the elastic design, $\delta = 0.875$ represents the most common case for beams in buildings due to the arrangements of variable actions, and $\delta = 0.75$ represents the common limit of the redistribution factor with equal quantities of reinforcement in spans and supports. Two structural systems were selected: interior span and end span, of a continuous beam or one-way continuous slab or a two-way spanning slab continuous over one long side. Two concrete types were chosen to cover the normal (NSC) and high (HSC) strength types of concrete. Fig. 6 exhibits the supports and reinforcement distribution.

The total mechanical reinforcement ratio is equal to the sum of mechanical reinforcement ratios on the span (sp) and half of the sum of two supports (sup) (given in Eq. (4) and Eq. (5)). Only considering this sum as constant, it is possible, with a small error, to change the redistribution factor without modifying the load capacity of the beam, when the redistribution factor is the changeable parameter. Table 2 shows the distribution of steel reinforcement along the beam for every combination between the redistribution factor δ and total mechanical reinforcement ratio ω^t. For all combinations and cross-sections, the mechanical compressive reinforcement ratio was taken as 50% of the mechanical tensile reinforcement ratio.

$$\text{Interior span: } \omega^t = \omega_{sp} + \frac{1}{2}\cdot(\omega_{sup} + \omega_{sup}) = \frac{A_s^{sp}\cdot f_y}{b\cdot d\cdot f_c} + \frac{A_s^{sup}\cdot f_y}{b\cdot d\cdot f_c} \quad (4)$$

$$\text{End span: } \omega^t = \omega_{sp} + \frac{1}{2}\cdot(\omega_{sup} + 0) = \frac{A_s^{sp}\cdot f_y}{b\cdot d\cdot f_c} + \frac{1}{2}\cdot\frac{A_s^{sup}\cdot f_y}{b\cdot d\cdot f_c} \quad (5)$$

2.4. Numerical model

According to the previous section, 324 continuous beams needed to be computed until collapse. To do this, a numerical model which applies the non-linear finite element method is developed to compute the strains and stresses along the beams during the loading.

Each beam was divided into several Bernoulli beam type elements with a length similar to 0.6h, according to the definition of plastic hinge length in MC2010 and EC2 (Fig. 4). One integration point per element was used. The computations performed showed the formation of plastic hinges on the expected elements. Fig. 7 illustrates the finite element meshes used for the analysis of the two structural systems. The analysis was implemented by loading increments.

For each loading increment, an iterative process is implemented to calculate the following parameters: i) nodal displacements, ii) element strains, iii) element stresses, iv) element stiffness by considering an accurate cross-section analysis and integrating in the element domain, v) new internal forces and vi) the residual forces. The iterative process stops when the residual forces are almost null. At the end of each loading increment, the plastic rotation of each element is calculated. The analysis stops when in any one element the plastic rotation is higher than the rotation capacity. This methodology works very well and gives precise results if the loading increments are small enough.

Figs. 8 and 9 exhibit the stress–strain relationships considered for reinforcing steel B500C and concrete C20 and C70, respectively, and used in the cross-section analysis. For concrete in compression, the

Table 1
Parameters studied and their values.

Parameter	Values
Span of the beam - l [m]	5 / 10 / 20
Effective depth of the cross-section - d [m]	0.25 / 0.45 / 0.95
Total mechanical reinforcement ratio - ω^t	0.2 / 0.4 / 0.6
Redistribution factor - δ	1.0 / 0.875 / 0.75
Structural system	Interior span / End span
Concrete	C20 / C70

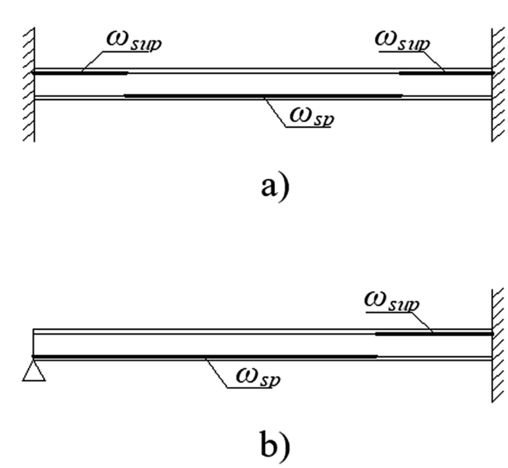

Fig. 6. Structural systems and distribution of reinforcement: (a) interior span, (b) end span.

Table 2
Distribution of reinforcing steel.

δ	ω^t	Interior span		End span	
		ω^{sp}	ω^{sup}	ω^{sp}	ω^{sup}
1.0	0.2	0.066	0.133	0.106	0.188
	0.4	0.133	0.267	0.212	0.376
	0.6	0.200	0.400	0.318	0.564
0.875	0.2	0.083	0.117	0.117	0.166
	0.4	0.167	0.233	0.234	0.332
	0.6	0.250	0.350	0.351	0.498
0.75	0.2	0.100	0.100	0.128	0.145
	0.4	0.200	0.200	0.256	0.290
	0.6	0.300	0.300	0.384	0.435

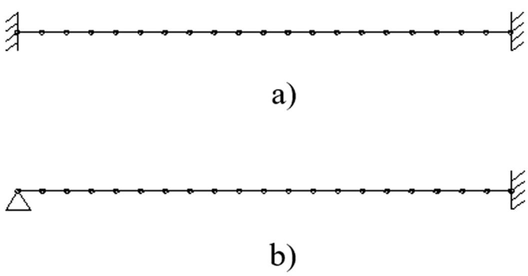

Fig. 7. Geometry meshes and supports: (a) interior span, (b) end span.

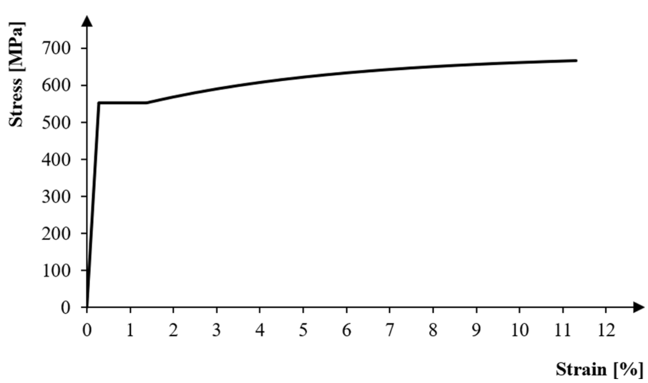

Fig. 8. Stress–strain relationship for reinforcing steel B500C [44].

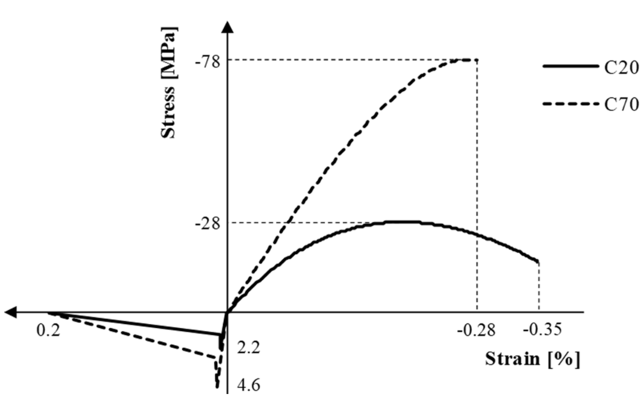

Fig. 9. Stress–strain relationship for the two concretes used.

MC2010 and EC2 parabolic model was applied and for concrete in tension the tension–stiffening law developed by Figueiras [43] was adopted.

3. Results and discussion

3.1. Deflection ductility index

Fig. 10 shows the typical results obtained by this numerical study for a beam or one-way spanning slab with $l = 5$ m, $d = 0.25$ m, $\delta = 1.0$, C20 and various mechanical reinforcement ratios. As expected, Δ_u decreases while Δ_y increases with the increase of total mechanical reinforcement ratio ω^t.

The deflection ductility indexes were computed for the 324 studied combinations. Fig. 11 shows the deflection ductility index as a function of slenderness ratio l/d and total mechanical reinforcement ratio ω^t for the two structural systems and for the two types of concrete. In these figures the plane surface for $\mu_\Delta = 1.0$ represents the limit from which the structures reach the ultimate deflection Δ_u without reaching its total design loading capacity, as explained in Section 2.2.

To obtain the final results in Fig. 11, the method of least squares was applied to smooth out some divergent values resulting from the computing process and to interpolate and to extrapolate for other values of the parameters. During the early analysis of the ductility index achieved from the variation of different parameters, it was noticed that the influence of the effective depth d and span l could be considered by only one parameter, the slenderness ratio l/d. Therefore, one parameter could be removed, and this fact allowed all the results to be viewed in 3D diagrams (Fig. 11).

The shape of the results for the two structural systems was similar for the same type of concrete. In fact, it was noticed that the shape of the deflection ductility index μ_Δ practically does not depend on the structural system. On the other hand, the slenderness ratio l/d, the redistribution factor δ, the type of concrete (NSC or HSC) and the total mechanical reinforcement ratio ω^t show relevant influence.

As expected: i) the deflection ductility index μ_Δ reduces with the increase of slenderness ratio l/d because with the increase of l/d the demand for plastic rotation increases faster than the rotation capacity; ii) the deflection ductility index μ_Δ reduces with the reduction of redistribution factor δ because more plastic rotation is required in the support plastic hinges (see Fig. 12), iii) the deflection ductility index μ_Δ reduces with the increase of the concrete strength class because the ultimate compressive strain of the concrete decreases; iv) the deflection ductility index μ_Δ reduces with the increase of total mechanical reinforcement ratio ω^t because the rotation capacity decreases with the increase of the relative depth of the compression zone, that is, with the mechanical reinforcement ratio.

These numerical results were obtained with the formulation of MC2010 and EC2 for the rotation capacity, which includes a margin of safety. For this reason, the results obtained here for the deflection ductility index, approximately between 0.5 and 3.5, are slightly smaller than the average experimental results found in the literature [26,30,45,46]. Taking this into account, the numerical results calculated

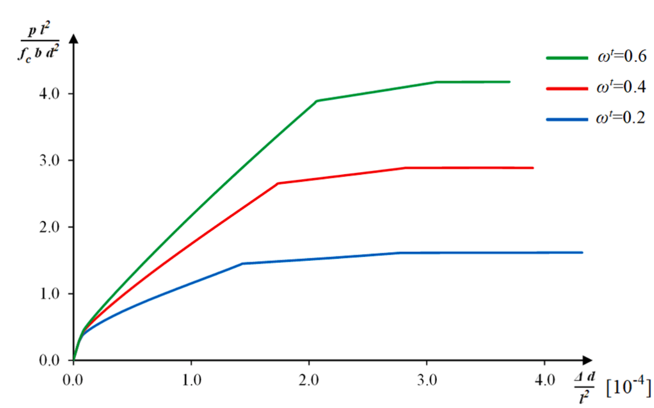

Fig. 10. Results for interior span with $l = 5$ m, $d = 0.25$ m, $\delta = 1.0$ and C20.

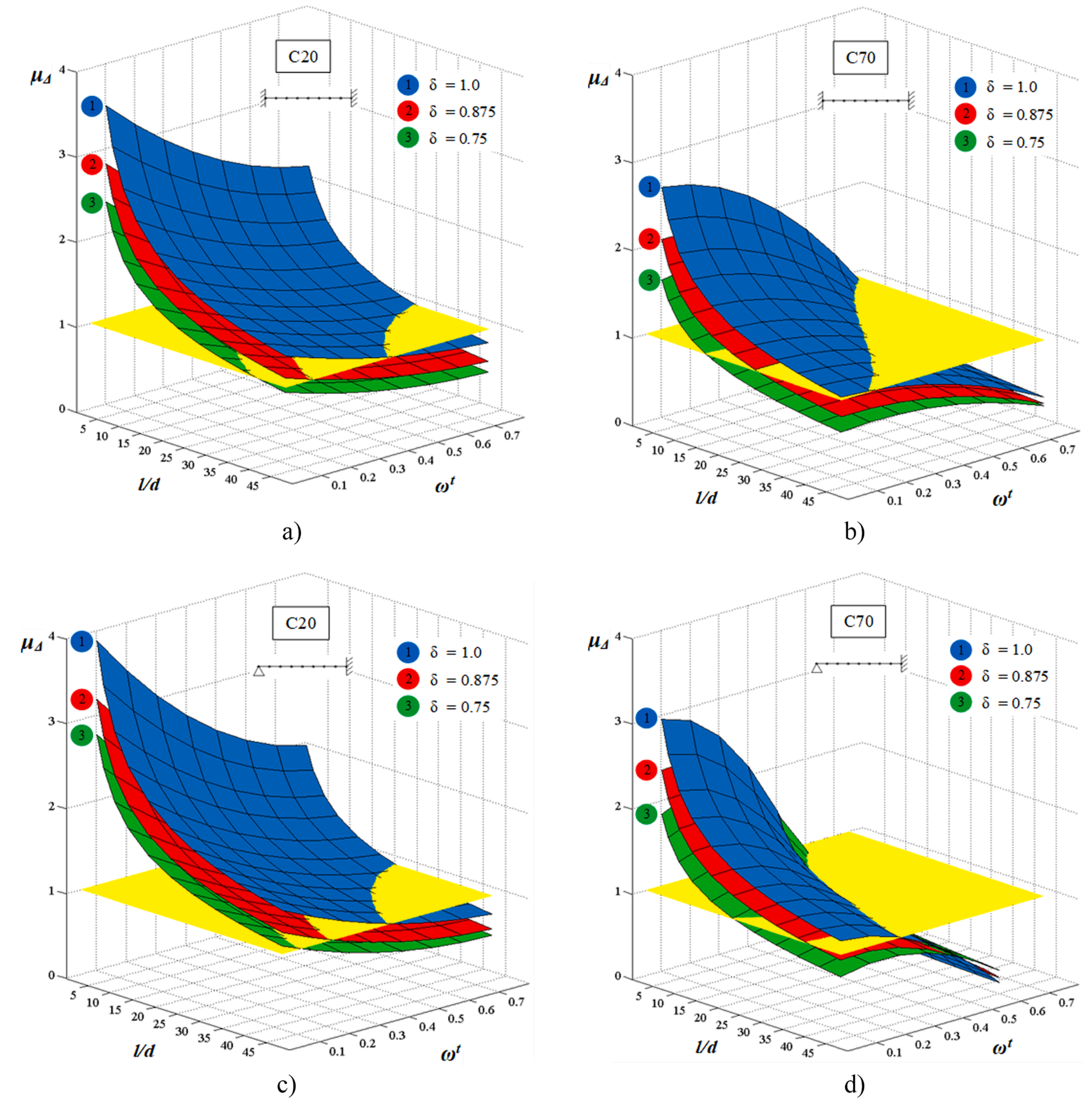

Fig. 11. Deflection ductility index: (a) interior span and concrete C20, (b) interior span and concrete C70, (c) end span and concrete C20, (d) end span and concrete C70.

here should be understood as the minimum characteristic values for the deflection ductility index expected for continuous beams or slabs.

Besides that, the great majority of experimental tests in the literature refer to simply supported beams, where the deflection ductility index can be considerably larger than the values obtained for continuous beams. In addition, many of these old experimental tests used reinforcing bars different from actuality, which means that the comparison of the results of those experimental tests with the results of this numerical study should be treated with caution.

3.2. *Span-to-depth ratio limits based on required ductility*

As explained in Section 2.2, the span-to-depth ratio limits based on the required ductility can be achieved from the deflection ductility index. These limits correspond to the intersection of the horizontal plan $\mu_\Delta = 1$ with the surfaces of the deflection ductility index represented in Fig. 11. These intersections are represented in Fig. 13, from which it is now easy to get the maximum slenderness ratio for a continuous beam or one-way spanning slab based on the required ductility.

The span-to-depth ratio limits depend on the total mechanical reinforcement ratio ω^t, the redistribution factor δ, the concrete strength class and the structural system. The reasons why the span-to-depth ratio limit

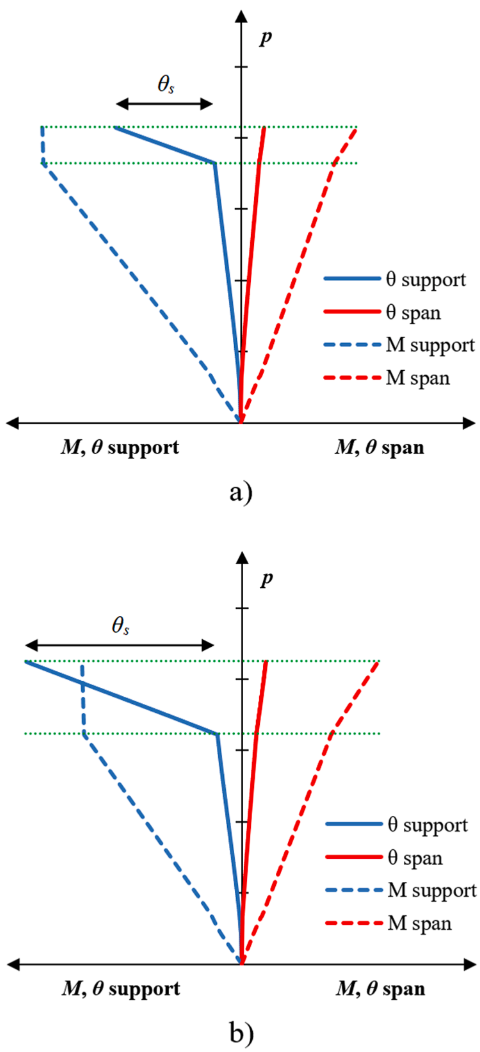

Fig. 12. Bending moment versus loading curve, rotation versus loading curve and plastic rotation, for the end span of a continuous beam or slab: (a) $\delta = 1.00$, (b) $\delta = 0.75$.

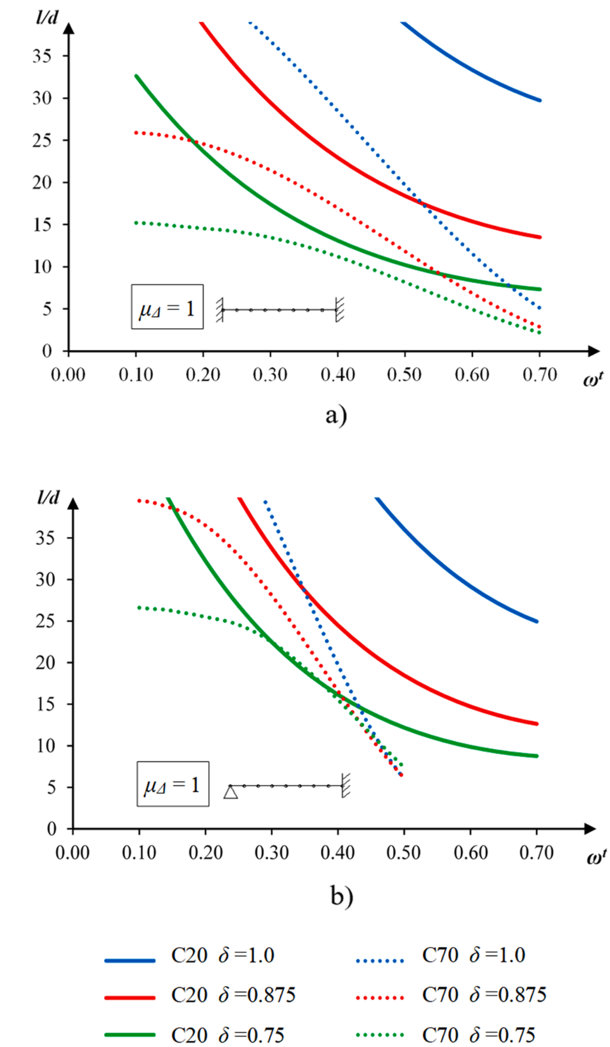

Fig. 13. Span-to-depth ratio limits based on required ductility: (a) interior span, (b) end span.

decreases with these four parameters are the same as detailed in the previous section for the deflection ductility index. The curves presented are relatively similar for the two structural systems when the same concrete strength class is considered. This means that the concrete strength is more relevant than the structural system.

In order to use NSC in reinforced concrete structures, some considerations should be pointed out. For the current beams in buildings ($\delta \geq 0.875$, $10 < l/d < 20$), only when $\omega^t > 0.45$, it may be required to reduce the beam slenderness from $l/d = 20$ to $l/d = 10$. For typical slabs ($\delta = 0.75$, $\omega^t < 0.3$) in general, it is safe if slenderness $l/d \leq 20$, but if a high percentage of the total mechanical reinforcement ratio (ω^t) is used (for example, a wide beam inside a slab due to architectural restrictions), the slenderness needs to be reduced or the redistribution factor (δ) increased.

In order to apply the HSC in reinforced structures, the values obtained here for the slenderness ratio could be restrictive for high values of the total mechanical reinforcement ratio. However, the geometrical reinforcement ratio in HSC is two to three times higher than NSC for the same total mechanical reinforcement ratio, which means that, for the same geometrical reinforcement ratios, the values of the total mechanical reinforcement ratio used in HSC are generally smaller than NSC. From this standpoint, the application of HSC in reinforced structures is encouraged.

According to MC2010 [1] and EC2 [2]: "Plastic analysis without any direct check of rotation capacity may be used for the ultimate limit state if … all the following are fulfilled: i) the area of tensile reinforcement is limited such that, at any section $x_u/d \leq 0.25$ for concrete strength classes ≤ C50/60, ii) reinforcing steel is either Class B or C, iii) the ratio of the moments at intermediate supports to the moments in the span should be between 0.5 and 2". Condition i) in this context is approximately similar to $\omega^t < 0.25$, condition ii) is satisfied in this paper, but if reinforcing steel of Class B were used the rotation capacity would be lower, and consequently the span-to-depth ratio limits would be lower, condition iii) in this context is similar to $\delta \geq 0.5$. Considering the results of Fig. 13: i) for $\delta = 1.0$, the MC2010 and EC2 conditions are enough, ii) for $\delta = 0.75$, the MC2010 and EC2 conditions are only valid if $l/d < 20$, and iii) for $\delta = 0.5$ (not computed in this work), the MC2010 and EC2 conditions will certainly be valid only for small span-to-depth ratios. For reinforcing steel of Class B the span-to-depth ratios would be more restricted. So, this suggests that the MC2010 and EC2 conditions are actually incomplete, unsafe and need to be revised.

As explained in the previous section, the numerical results calculated here should be understood as the minimum characteristic values for the span-to-depth ratio limits. This means that not all the continuous beams or slabs identified in the last paragraph are potentially unsafe, but only a small percentage of them.

3.3. Comparison between ductility and deflection span-to-depth ratio requirements

In the current practice of pre-design of beams and slabs, it is usual to condition the dimensions of the beams and slabs in such a way that the SLS related to the deflection control is automatically fulfilled. However, Fig. 13 showed curves that may also be of practical interest in the pre-design of continuous beams and slabs, if the engineer wants these elements to reach failure with enough ductility. In this section, the results obtained by these two different methodologies are compared.

Note that both pre-design methodologies are in accordance with the principles of MC2010 and EC2. Deflection control is defined explicitly, while the required ductility is defined implicitly through the rotation capacity. Therefore, the study carried out here is a comparison of methodologies obtained according to the same code, to be consistent, although they come from different limit states.

According to MC2010 [1] and EC2 [2], if beams or slabs are designed in order to fulfil the l/d ratio limits defined in Eqs. (6) and (7), it is expected that the respective deflection will not exceed the limits defined in these codes.

$$\frac{l}{d} = K\cdot\left[11 + 1.5\sqrt{f_{ck}}\cdot\frac{\rho_0}{\rho} + 3.2\sqrt{f_{ck}}\cdot\left(\frac{\rho_0}{\rho}-1\right)^{1.5}\right] if\,\rho \le \rho_0 \qquad (6)$$

$$\frac{l}{d} = K\cdot\left[11 + 1.5\sqrt{f_{ck}}\cdot\frac{\rho_0}{\rho-\rho'} + \frac{1}{12}\sqrt{f_{ck}}\cdot\sqrt{\frac{\rho'}{\rho_0}}\right] if\,\rho > \rho_0 \qquad (7)$$

where: l/d is the span-to-depth ratio limit; K is a factor to take into account the different structural systems; $\rho_0 = 10^{-3}\sqrt{f_{ck}}$ is the reference reinforcement ratio; ρ is the required tension reinforcement ratio at mid-span to resist the moment due to the design loads; ρ' is the required compression reinforcement ratio at mid-span to resist the moment due to design loads; f_{ck} [MPa] is the characteristic compressive strength of concrete.

Fig. 14 compares the two pre-design methodologies for the two structural systems and for the two concrete classes.

For normal strength concrete, the current pre-design method based on the slenderness limits of the deflection control is only valid if the redistribution factor δ is higher than approximately 0.9; below this value, the required ductility is more restricted than deflection control, especially for beams (high values of total mechanical reinforcement ratio ω^t), where the slenderness limits may be only half of the values given by deflection control.

For high strength concrete, the required ductility is almost always the most restricted condition. For high values of total mechanical reinforcement ratio ω^t the difference is huge. These results show that the application field of the high strength concrete could be more limited than initially thought.

The curves related to the deflection control in Fig. 14 also enable us to answer a pertinent question in the study of structural ductility, but which does not always have a properly validated answer. According to the literature [26], deflection control is not as sensitive as crack control when moment redistribution is applied. However, the curves for deflection control in Fig. 14 indicate that there is some influence of the redistribution factor in the span-to-depth ratio limits, mainly in the interior span.

3.4. Proposed formula for general span-to-depth ratio limits

The results presented in the previous section show the relevance of developing pre-design equations that include the requirements of deflection control and the required ductility. Thus, this section presents equations which satisfy both requirements.

To achieve this, several steps were done with the results of Fig. 14: i) in each figure a linear envelope of the two requirements was calculated for each δ, ii) for each figure a regression surface was defined in order to

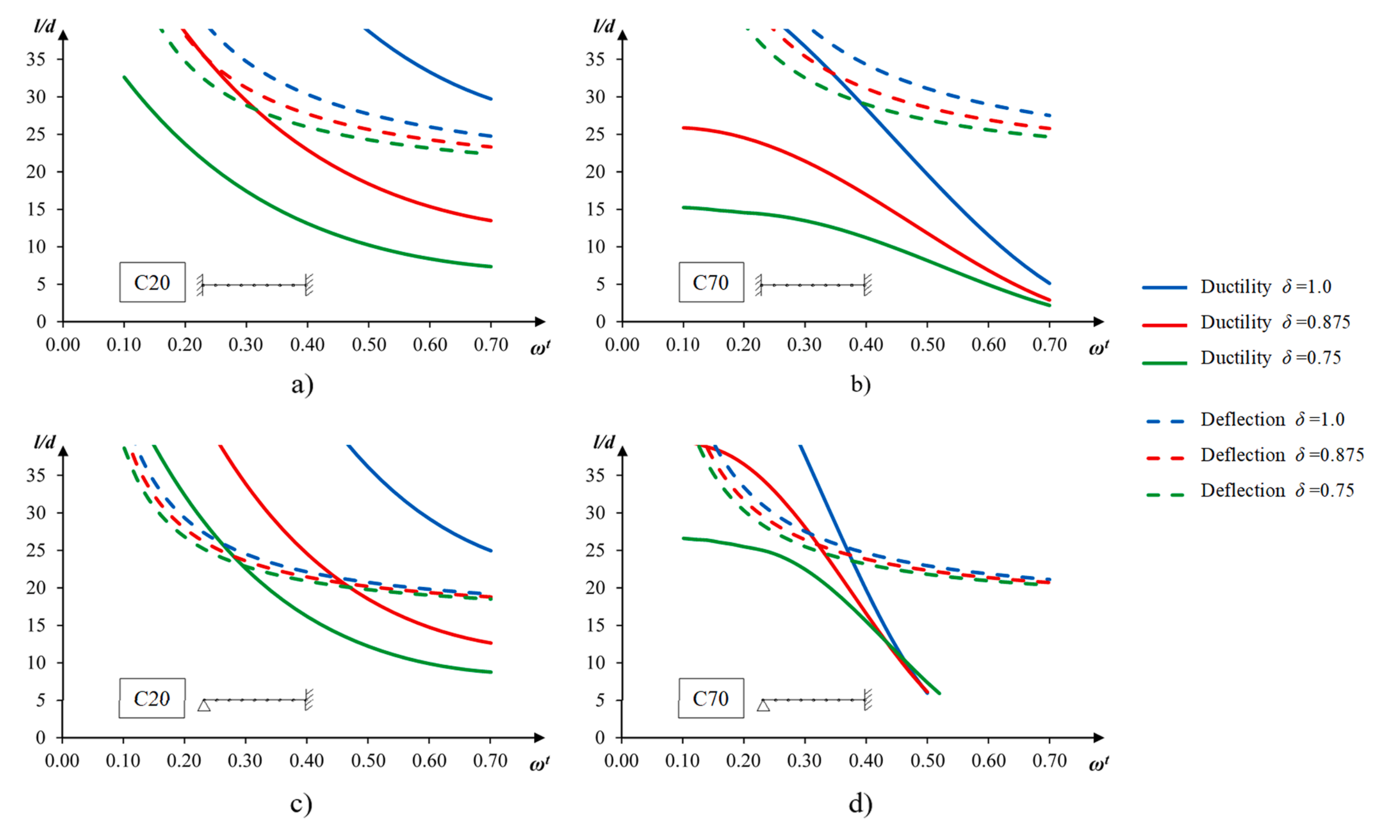

Fig. 14. Comparison between span-to-depth ratio limit requirements: (a) interior span and concrete C20, (b) interior span and concrete C70, (c) end span and concrete C20, (d) end span and concrete C70.

simulate all their three envelopes with one equation, that is $l/d\ (\delta, \omega^t)$, iii) for each structural system the two regression surfaces (C20 and C70) were joined, making a linear transition between them (Fig. 14a and b) for interior span, and Fig. 14c and d) for end span) to make two 4D surfaces, which correspond to the final equations, that is $l/d\ (\delta, \omega^t, f_{ck})$.

Eqs. (8)–(11), which correspond to step ii), are the span-to-depth ratio limits for each subfigure of Fig. 14. These linear expressions depend only on redistribution factor δ and total mechanical reinforcement ratio ω^t.

$$\text{Interior span and concrete C20}: \frac{l}{d} = -22.8 + 68\cdot\delta - 34\cdot\omega^t \quad (8)$$

$$\text{Interior span and concrete C70}: \frac{l}{d} = -94.3 + 152\cdot\delta + 131\cdot\omega^t \quad (9)$$

$$\text{End span and concrete C20}: \frac{l}{d} = 33.0 - 86\cdot\omega^t + 64\cdot\delta\cdot\omega^t \quad (10)$$

$$\text{End span and concrete C70}: \frac{l}{d} = -2.0 + 15\cdot\omega^t - 108\cdot\delta\cdot\omega^t + 56\cdot\delta \quad (11)$$

Eqs. (12) and (13), which correspond to step iii), are the final span-to-depth ratio limits for interior span and end span structural systems, respectively. They allow us to pre-design continuous beams or one-way spanning slabs of current buildings satisfying the deflection control and structural ductility requirements.

$$\frac{l}{d} = 6 + 34.4\cdot\delta - 1.43\cdot f_{ck} - 100\cdot\omega^t + 1.68\cdot\delta\cdot f_{ck} + 83.2\cdot\delta\cdot\omega^t + 3.31\cdot f_{ck}\cdot\omega^t - 4.16\cdot\delta\cdot f_{ck}\cdot\omega^t \quad (12)$$

$$\frac{l}{d} = 46 - 22.4\cdot\delta - 0.70\cdot f_{ck} - 126\cdot\omega^t + 1.12\cdot\delta\cdot f_{ck} + 133\cdot\delta\cdot\omega^t + 2.01\cdot f_{ck}\cdot\omega^t - 3.44\cdot\delta\cdot f_{ck}\cdot\omega^t \quad (13)$$

where: $5 < l/d < 50$ is the span-to-depth ratio limit; $0.7 < \delta < 1.0$ is the redistribution factor, $10 < f_{ck}$ [MPa] < 100 is the characteristic compressive strength of concrete, and $0.1 < \omega^t < 0.7$ is the total mechanical reinforcement ratio.

Fig. 15 presents a comparison between the proposed limit for an interior span and concrete C30 with several existing deflection limits in different codes and two recent proposals in the literature (Caldentey et al. [13] and Marí et al. [14]). It should be mentioned that while the equations of the codes are easier to work (fewer parameters), the equations of the two proposals are harder to work (more parameters: shrinkage, creep, dead versus live load, etc.), which makes it almost impossible to produce curves for exactly the same conditions. In this way, to avoid mistakes in plotting Fig. 15, the results of the simulations presented in Fig. 3 of Caldentey et al. [13] (C30/37, DL-LL = 60%-40%) and in Fig. 4b of Marí et al. [14] (p/b = 25kN/m^2) were used. These curves seemed to be the most plausible to apply in current building beams. So, although all the curves are not exactly comparable, it can be concluded from Fig. 15 that for $\delta = 1.00$ (without redistribution), the proposed limit is in line with the existing limits because deflection control is the most restrictive condition, while for $\delta = 0.75$ (with high redistribution), the proposed limit presents much lower values because the required ductility is the most restrictive condition.

4. Conclusions

The increasing complexity in the design of RC structures has motivated the search for new simplified methods that could help engineers to easily define structural solutions that fulfil the complex rules. Particularly, the span-to-depth (or slenderness) ratio limits are very useful for the pre-design of beams and slabs.

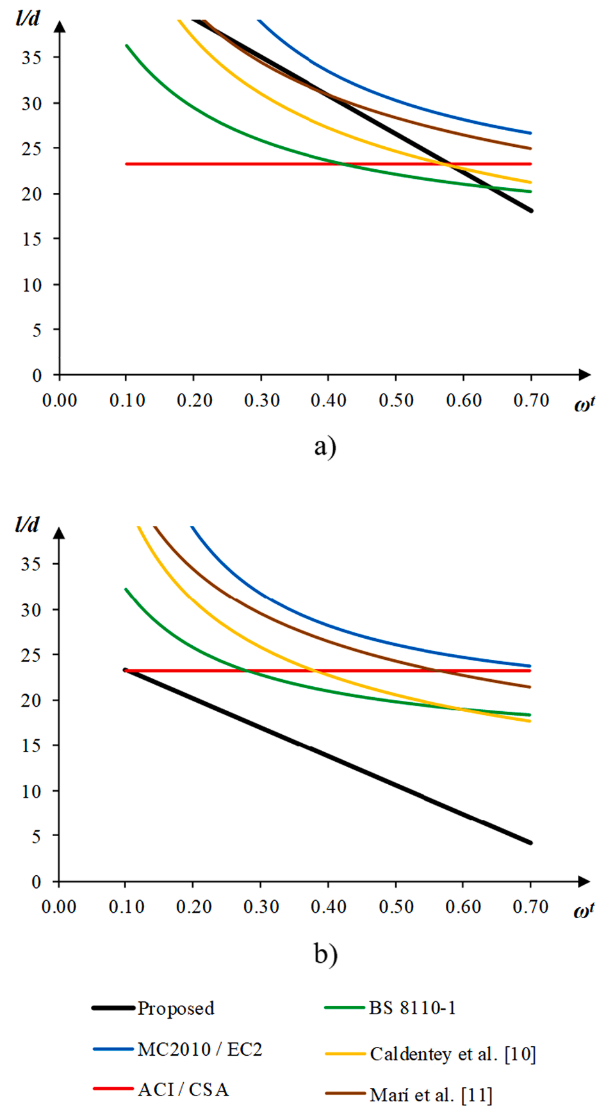

Fig. 15. Comparison between proposed and several deflection span-to-depth ratio limits, for interior span and concrete C30: (a) $\delta = 1.00$, (b) $\delta = 0.75$.

One of the topics that concern engineers during the design of RC structures, in relation to other materials is the reduced ductility of the RC elements. In fact, fragile and premature rupture can occur on continuous beams and slabs if the rotation capacity is insufficient. To avoid that, the plastic rotations that occur in hinges needed to be checked during the design. However, this process requires non-linear structural analysis, which is usually not performed during the structural design of buildings. The work presented in this paper allows this hard task to be avoided by using a simplified method based on span-to-depth ratio limits.

To achieve this, a numerical study which performed the non-linear structural analysis of 324 continuous beams (or one-way continuous slabs) until rupture was carried out. The parameters considered were: span l, effective depth of the cross-section d, total mechanical reinforcement ratio ω^t, redistribution factor δ, structural system (end/interior span) and concrete strength class f_{ck}. From this study, the deflection ductility indexes were plotted. With these results, the boundary between fragile and ductile cases could be established, making it possible to define the span-to-depth ratio limits for the required ductility.

From this study the following conclusions can be pointed out:

- The results obtained for the deflection ductility index μ_{Δ}, between 0.5 and 3.5, are mainly acceptable, but also indicate several beams without enough ductility ($\mu_{\Delta} < 1$). The deflection ductility index μ_{Δ} reduces with the increase of: the slenderness ratio l/d, concrete strength class f_{ck} and total mechanical reinforcement ratio ω^{t}. The deflection ductility index μ_{Δ} also reduces with the reduction of the redistribution factor δ.
- The span-to-depth ratio limits for ductility requirements change with the variation of several parameters in the same way as described above for the deflection ductility index. The limit values for high strength concrete are very restricted, so using a high mechanical reinforcement ratio in this type of concrete is not recommended.
- Considering the practical application of these limits in buildings: i) for the current beams ($\delta \geq 0.875$, $10 < l/d < 20$), only when $\omega^{t} > 0.45$ it may be required to reduce the beam slenderness from $l/d = 20$ to $l/d = 10$; ii) for typical slabs ($\delta = 0.75$, $\omega^{t} < 0.3$), in general, it is safe if slenderness $l/d \leq 20$, however, if a high percentage of total mechanical reinforcement ratio (ω^{t}) is used, the slenderness (l/d) needs to be reduced or the redistribution factor (δ) increased.
- Considering the validity of the conditions of MC2010 [1] and EC2 [2] to use plastic analysis without any direct check of rotation capacity: i) for $\delta = 1.0$, the conditions are sufficient; ii) for $\delta = 0.75$, the conditions are only valid if $l/d < 20$; and iii) for $\delta = 0.5$, although not computed in this work, the conditions will certainly be valid only for small span-to-depth ratios. In addition, for reinforcing steel of Class B the span-to-depth ratios will be more restricted. Therefore, this suggests that the conditions of MC2010 [1] and EC2 [2] are actually incomplete, unsafe and need to be revised.
- The usual methodology of controlling the ductility of continuous beams and slabs by indirectly limiting the redistribution factor (δ) and the relative depth of the compression zone (x/d) is not enough. The results suggest that the element slenderness ratio (l/d) should also be considered.
- Regarding the comparison between the ductility and deflection span-to-depth ratio limits: i) for normal strength concrete, when the redistribution factor δ is lower than approximately 0.9, the required ductility is the most restricted condition; ii) for high strength concrete, the required ductility is almost always the most restricted condition.
- New span-to-depth ratio limits were presented in Eqs. (12) and (13), which fulfil both the required ductility and deflection control requirements. These limits depend on the structural system, the redistribution factor δ, the characteristic compressive strength of concrete f_{ck} and the total mechanical reinforcement ratio ω^{t}.
- From the results presented here and code (MC2010 and EC2) analysis, it can be inferred that there are several constructed buildings whose continuous beams and slabs do not have sufficient ductility. However, as this problem is only noticed near failure and the service loading is lower by enough than the ultimate loading, building collapse is rare and generally results from excessive or unexpected loading, and the problem is generally undetected by people and engineers. Nevertheless, the problem exists.

To conclude, it is expected that this paper will motivate researchers to look again at the ductility of RC structures, and the ongoing revision of MC2010 [1] and EC2 [2] could benefit from these results.

CRediT authorship contribution statement

José Santos: Conceptualization, Methodology, Software, Validation, Writing - original draft. **António Abel Henriques:** Conceptualization, Resources, Writing - review & editing, Supervision, Funding acquisition.

Declaration of Competing Interest

The authors declare that they have no known competing financial interests or personal relationships that could have appeared to influence the work reported in this paper.

Acknowledgments

This work was financially supported by: Base Funding - UIDB/04708/2020 of the CONSTRUCT - Instituto de I&D em Estruturas e Construções - funded by national funds through the FCT/MCTES (PIDDAC).

References

[1] fib. Bulletin 56 - Model Code 2010 - First complete draft, Volume 2. Lausanne, Switzerland: International Federation for Structural Concrete (fib); 2010.
[2] EN 1992-1-1. Eurocode 2: Design of concrete structures - Part 1-1: General rules and rules for buildings. Brussels, Belgium: European Committee for Standardization; 2004.
[3] Marí AR, Bairán JM, Duarte N. Long-term deflections in cracked reinforced concrete flexural members. Eng Struct 2010;32:829–42. https://doi.org/10.1016/j.engstruct.2009.12.009.
[4] Gribniak V, Cervenka V, Kaklauskas G. Deflection prediction of reinforced concrete beams by design codes and computer simulation. Eng Struct 2013;56:2175–86. https://doi.org/10.1016/j.engstruct.2013.08.045.
[5] Bertero R, Bertero A. Statistical evaluation of minimum thickness provisions for slab deflection control. ACI Struct J 2018;115:1659–70. https://doi.org/10.14359/51706926.
[6] Gardner NJ. Span/thickness limits for deflection control. ACI Struct J 2011;108:453–60. https://doi.org/10.14359/51682985.
[7] Lee YH, Kim MS, Lee J, Scanlon A. Comparison of minimum thickness provisions for concrete beams in building codes and standards. Can J Civ Eng 2013;40:595–602. https://doi.org/10.1139/cjce-2012-0479.
[8] Slavchev SV, Guglev SR. Analysis and recommendations about EN1992-1-1 formulas for limiting the span/depth ratio. Appl Mech Mater 2015;769:273–80. https://doi.org/10.4028/www.scientific.net/AMM.769.273.
[9] Eren T, Dancygier AN. Evaluation of span-to-depth ratio provisions for deflection control of one-way RC construction. Structures 2020;25:696–707. https://doi.org/10.1016/j.istruc.2020.03.035.
[10] Young Hak L, Andrew S. Comparison of one- and two-way slab minimum thickness provisions in building codes and standards. ACI Struct J 2010;107.
[11] Debernardi PG, Taliano M. Span-to-height ratio limits for prestressed concrete members. Struct Concr 2010;11:35–43. https://doi.org/10.1680/stco.2010.11.1.035.
[12] Scanlon A, Lee YH. Unified span-to-depth ratio equation for nonprestressed concrete beams and slabs. ACI Struct J 2006;103:142–8. https://doi.org/10.14359/15095.
[13] Caldentey AP, Cembranos JM, Peiretti HC. Slenderness limits for deflection control: A new formulation for flexural reinforced concrete elements. Struct Concr 2017;18:118–27. https://doi.org/10.1002/suco.201600062.
[14] Marí A, Torres L, Oller E, Barris C. Performance-based slenderness limits for deformations and crack control of reinforced concrete flexural members. Eng Struct 2019;187:267–79. https://doi.org/10.1016/j.engstruct.2019.02.045.
[15] Matamoros AB, Sozen MA. Drift limits of high-strength concrete columns subjected to load reversals. J Struct Eng 2003;129:297–313. https://doi.org/10.1061/(ASCE)0733-9445(2003)129:3(297).
[16] Lam SSE, Wu B, Wong YL, Wang ZY, Liu ZQ, Li CS. Drift capacity of rectangular reinforced concrete columns with low lateral confinement and high-axial load. J Struct Eng 2003;129:733–42. https://doi.org/10.1061/(ASCE)0733-9445(2003)129:6(733).
[17] Rodrigues H, Varum H, Arêde A, Costa A. A comparative analysis of energy dissipation and equivalent viscous damping of RC columns subjected to uniaxial and biaxial loading. Eng Struct 2012;35:149–64. https://doi.org/10.1016/j.engstruct.2011.11.014.
[18] Wibowo A, Wilson JL, Lam NTK, Gad EF. Drift performance of lightly reinforced concrete columns. Eng Struct 2014;59:522–35. https://doi.org/10.1016/j.engstruct.2013.11.016.
[19] Del Zoppo M, Di Ludovico M, Verderame Gerardo M, Prota A. Experimental behavior of nonconforming RC columns with deformed bars under constant axial load and fixed biaxial bending. J Struct Eng 2017;143:04017153. https://doi.org/10.1061/(ASCE)ST.1943-541X.0001892.
[20] Raza S, Menegon SJ, Tsang H-H, Wilson JL. Force-displacement behavior of limited ductile high-strength RC columns under bidirectional earthquake actions. Eng Struct 2020;208:110278. https://doi.org/10.1016/j.engstruct.2020.110278.
[21] Sindel Z, Akbaş R, Tezcan SS. Drift control and damage in tall buildings. Eng Struct 1996;18:957–66. https://doi.org/10.1016/0141-0296(95)00215-4.
[22] Erduran E, Yakut A. Drift based damage functions for reinforced concrete columns. Comput Struct 2004;82:121–30. https://doi.org/10.1016/j.compstruc.2003.10.003.
[23] Lu Y, Gu X, Guan J. Probabilistic drift limits and performance evaluation of reinforced concrete columns. J Struct Eng 2005;131:966–78. https://doi.org/10.1061/(ASCE)0733-9445(2005)131:6(966).

[24] Woods JM, Kiousis PD, Ehsani MR, Saadatmanesh H, Fritz W. Bending ductility of rectangular high strength concrete columns. Eng Struct 2007;29:1783–90. https://doi.org/10.1016/j.engstruct.2006.09.024.
[25] CEB. Ductility - Reinforcement, Bulletin d'Information 218. Lausanne: Comité Euro-International du Béton; 1993.
[26] CEB. Ductility of reinforced concrete structures, Bulletin d'Information 242. Lausanne: Comité Euro-International du Béton; 1998.
[27] Bernardo LFA, Lopes SMR. Neutral axis depth versus flexural ductility in high-strength concrete beams. J Struct Eng 2004;130:452–9. https://doi.org/10.1061/(ASCE)0733-9445(2004)130:3(452).
[28] Bagge N, O'Connor A, Elfgren L, Pedersen C. Moment redistribution in RC beams – A study of the influence of longitudinal and transverse reinforcement ratios and concrete strength. Eng Struct 2014;80:11–23. https://doi.org/10.1016/j.engstruct.2014.08.029.
[29] Sin LH, Huan WT, Islam MR, Mansur MA. Reinforced lightweight concrete beams in flexure. ACI Struct J 2011;108:3–12. https://doi.org/10.14359/51664197.
[30] Carmo RNF. Rotação Plástica e Redistribuição de Esforços em Vigas de Betão de Alta Resistência. Tese de Doutoramento, Departamento de Engenharia Civil, Faculdade de Ciências e Tecnologia, Universidade de Coimbra: Coimbra, Portugal; 2004.
[31] Shin SW, Kamara M, Ghosh SK. Flexural Ductility Strength Prediction and Hysteretic Behavior of Ultra-High-Strength Concrete Members. High-Strength Concrete, Second International Symposium. ACI1990.
[32] Bernardo L, Nepomuceno M, Pinto H. Neutral axis depth versus ductility and plastic rotation capacity on bending in lightweight-aggregate concrete beams. Materials 2019;12:3479. https://doi.org/10.3390/ma12213479.
[33] Salvatore W, Buratti G, Maffei B, Valentini R. Dual-phase steel re-bars for high-ductile r.c. structures, Part 2: Rotational capacity of beams. Eng Struct 2007;29 (3333–41). https://doi.org/10.1016/j.engstruct.2007.09.003.
[34] Farouk MA, Khalil KF. Alternative mathematical modeling for plastic hinge of reinforced concrete beam. SN Appl Sci 2019;2:113. https://doi.org/10.1007/s42452-019-1684-9.
[35] Pokhrel M, Bandelt MJ. Plastic hinge behavior and rotation capacity in reinforced ductile concrete flexural members. Eng Struct 2019;200:109699. https://doi.org/10.1016/j.engstruct.2019.109699.
[36] Carpinteri A, Corrado M. Upper and lower bounds for structural design of RC members with ductile response. Eng Struct 2011;33:3432–41. https://doi.org/10.1016/j.engstruct.2011.07.007.
[37] Erduran E, Yakut A. Component damage functions for reinforced concrete frame structures. Eng Struct 2007;29:2242–53. https://doi.org/10.1016/j.engstruct.2006.11.003.
[38] Lopes SM, Carmo RNF. Deformable strut and tie model for the calculation of the plastic rotation capacity. Comput Struct 2006;84:2174–83. https://doi.org/10.1016/j.compstruc.2006.08.028.
[39] Haskett M, Oehlers DJ, Mohamed Ali MS, Wu C. Rigid body moment-rotation mechanism for reinforced concrete beam hinges. Eng Struct 2009;31:1032–41. https://doi.org/10.1016/j.engstruct.2008.12.016.
[40] Zhou KJH, Ho JCM, Su RKL. Normalised rotation capacity for deformability evaluation of high-performance concrete beams. Earthquake Struct 2010;1:269. https://doi.org/10.12989/eas.2010.1.3.269.
[41] Fusco R, Montuori R, Nastri E, Piluso V. Critical analysis of ultimate rotation formula for R.C. columns subjected to cyclic loadings. Eng Struct 2018;177 (160–74). https://doi.org/10.1016/j.engstruct.2018.09.065.
[42] Ho JC-M, Zhou KJ-H. Limited deformability design of high-strength concrete beams in low to moderate seismicity regions. J Civil Eng Manage 2011;17 (409–23). https://doi.org/10.3846/13923730.2011.594219.
[43] Figueiras J. Ultimate load analysis of anisotropic and reinforced concrete plates and shells. PhD Thesis. Swansea, United Kingdom: University of Wales:; 1983.
[44] ARCER TC. Characteristic Stress-Strain Curves for ARCER Mark Special Ductility Weldable Steel. Madrid: ARCER; 2003.
[45] McCarty CM. Behavior Of Two-Span Continous Reinforced Concrete Beams. Masteŕs Thesis, Ohio University: USA; 2008.
[46] Ventorini LA. Influência da Aderência na Capacidade de Rotação Plástica de Vigas de Concreto Armado. PhD Thesis, Universidade Federal do Rio de Janeiro: Rio de Janeiro, Brasil; 2003.